Grain growth simulation in an IF steel – Effect of grain boundary mobility

A Ayad, N Rouag, Francis Wagner

Grain growth simulation in an IF steel – Effect of grain boundary mobility

2015 IOP Conf. Ser.: Mater. Sci. Eng. 82 012051

(http://iopscience.iop.org/1757-899X/82/1/012051)

Grain growth simulation in an IF steel - Effect of grain boundary mobility

A Ayad[1,2] , N Rouag[2] and F. Wagner[3]
[1] Département de Pharmacie, Faculté de Médecine, Université Constantine 3, Algeria
[2]Laboratoire de Microstructures et Défauts dans les Matériaux,
Université Constantine 1, Algeria
[3]LEM3, (CNRS-UMR 7239), Université de Lorraine, Ile du Saulcy, 57045 Metz, France
E-mail: abdelhak_ayad@yahoo.com

Abstract. In a recent paper, we have proposed a modified Potts model for the simulation of the normal grain growth stage in an IF steel. An original concept is introduced by a modular consideration of the grain size effect. It is based on experimental observations of partial textures of certain (sub) populations of grains. This allowed both better reflect the pressure at the grain boundaries and significantly speed up the calculations. This model was used to reproduce the main features of the microstructure and texture. Improvement of texture behavior, especially of the component {111}<112>, which differs slightly from the experiment, requires the introduction of strong assumptions on energy and mobility of grain boundaries. The objective of this study is to verify the ability of the modified Monte Carlo model to give satisfactory results for grain growth, by considering various assumptions on energy and mobility of grain boundaries. The validity of such assumptions and their impact on the simulation results are analyzed and discussed.

1. Introduction

Due to their excellent deep drawability, a large amount of research work has been carried out to study the development of recrystallization texture and microstructure in IF steels [1-6]. Therefore, many attempts have been made to model the microstructure evolution during heat treatments [7-12]. In a recently published work by the present authors, a modified Potts model for the simulation of the normal grain growth stage in an IF steel has been proposed [13]. It allows both better reflect the pressure at the grain boundaries (GBs) and significantly speed up the calculations. This model, which uses isotropic GB mobility and Read-Shockley(R-S) GB energy, reproduces globally the main features of the microstructure and texture. However, the texture shows a small increase of the component C-{111}<112> which differs somewhat from the experimental evolution. Enhancement of texture behavior requires the introduction of realistic energy and mobility of GBs. Some of the drawbacks are that it requires material data which are often not available and must then be replaced by assumptions. The first attempts to include anisotropic grain properties into Potts MC model simulations dates back to the eighties [14,15]. Holm et al. [16] were the first to introduce an anisotropic energy and mobility for GBs, with a switching probability.

It has often been suggested [17,18] that during normal grain growth, selective growth of grains of some particular orientations is controlled by specific types of coincidence site lattice (CSL) boundaries. Recently the Potts model was further generalized to also include the GB characteristics of certain CSLs [19,20].

In this work, a modified 2D Potts Monte Carlo model including anisotropy of GB mobility (dependent on misorientation) including the CSL GBs has been used, and a systematic study of their effect on grain growth texture of IF steel has been carried out. Some attention is also paid to the possible role of certain Σ <111> GBs during grain growth.

2. Simulation procedure

We briefly recall here the main points of the Monte Carlo grain growth method. The simulation method uses an interaction energy E_i associated to each site i [16]:

$$E_i = \sum_{j=1}^{n} \gamma(\theta_{ij}), \quad (1)$$

where γ, θ_{ij} and n are the energy per unit area of GB, the misorientation angle and number of neighbours of the selected site i, respectively. The total system energy is given by the sum over all lattice sites N.

The GB energy is defined by a Read-Shockley function with a cutoff angle $\theta^*=15°$:

$$\gamma_{RS}(\theta_{ij}) = \frac{\theta}{\theta^*}\left[1 - \ln\left(\frac{\theta}{\theta^*}\right)\right] \quad \text{if } \theta \le \theta^* \quad \text{and } \gamma_{RS}(\theta_{ij}) = 1 \quad \text{if } \theta > \theta^* \quad (2)$$

Simulation of grain growth involves the random selection of a site i and its neighbouring site j. The reorientation attempt is accepted with a probability P :

$$P = \frac{M(\theta_{ij})}{M_{max}} \frac{\gamma(\theta_{ij})}{\gamma_{max}} \quad \text{if } \Delta E \le 0 \quad \text{and } P = \frac{M(\theta_{ij})}{M_{max}} \frac{\gamma(\theta_{ij})}{\gamma_{max}} \exp\left(\frac{-\Delta E}{\beta\gamma(\theta_{ij})}\right) \quad \text{if } \Delta E > 0 \quad (3)$$

ΔE is the energy difference between altered and original state. The constants γ_{max} and M_{max} are the maximum allowed grain boundary energy and mobility, respectively. Both are equal to unity in these simulations. The constant β is an effective "lattice temperature" often chosen on an empirical basis. The mobility $M(\theta_{ij})$ is sometimes considered as being constant or can also follow an "S-curve" dependence on misorientation to give a sharp transition from low to high in the vicinity of the transition from low to high angle boundary type [21]. Both energy and mobility functions may include particular values for the CSL grain boundaries if data are available showing specific situations [10,22].

It is possible to increase the calculation speed by increasing the driving force in some specific situations. We have introduced such an effect in the following way. Instead of using the energy E_i associated to a site (see Eq. 1) we define a modified site energy E_i^*:

$$E_i^* = \frac{E_i}{(D_i/D_m)^p} \quad (4)$$

where E_i is the standard energy associated to a site number i (Eq. 1), D_i is the diameter of the grain to which the site i belongs and D_m is the mean diameter of the considered set of grains. This definition for E_i^* leads to favour the growth of large grains and, above all, to penalize the smallest grains. p is an empirical parameter which makes more or less effective this 'size effect' (p=0 suppresses it totally and corresponds then to the classical case whereas p=1 gives it the maximal influence). The motivation for such a modification as well as its consequences has been described in a previous work [13].

3. Experimental procedure

In this investigation, texture data were analyzed for an IF steels that had previously been studied [13, 23]. This IF steel was cold rolled up to 75% thickness reduction (final thickness 0.7 mm) and then submitted to an annealing treatment. The chemical composition of this steel is (% wt) :0.008 C, 0.2 Mn, 0.004 P, 0.01 S, 0.003N, 0.004 Si, 0.007 Cu, 0.02 Ni, 0.014 Cr, 0.04 Al, 0.1 Ti.

The data used here to start the simulation consist of an EBSD map made of such an IF sample heat treated at 630°C for 3 hours. A detailed study has shown that primary recrystallization is nearly finished for this heat treatment condition [23]. The map corresponds to a surface of 0.270 mm^2 which was obtained by using a JEOL 6490 FEG-SEM and an HKL EBSD system. The initial data set for the grain growth simulation is a set of 1 083 065 pixels taken as the lattice sites. This map corresponds to a set of 3104 grains, using a criterion of 5° misorientation to detect grains. When considering only grains with at least 4 pixels, 2982 grains with a size larger than 3 pixels are left. The mean grain size is 10.8 μm.

To compare the results obtained from simulations with experimental data, a second IF sample was heat treated at 800°C for 5 hours. The EBSD map contains 1 923 201 pixels, with

a total analyzed area of 0.480 mm². The map contains 1635 grains with an area larger than 3 pixels. This gives a mean grain size of 19.4 μm. It represents twice the initial value (initial means at the end of primary recrystallization).

4. Results and discussion

4.1. Experimental texture

The ODFs of the two samples, at the end of primary recrystallization and after grain growth, have been calculated from the individual orientations of the EBSD maps. ODF calculations have been made assuming cubic-orthorhombic symmetries. The main features appear in the φ_2=45° sections which are shown in Fig. 1. The texture mainly consists of a γ fiber with a relatively large spread around it, especially in the α fiber direction (i.e. for φ_1=0°). Inside this γ fiber the density is approximately evenly distributed with a slight peak around the orientation {111}<110> in the first case (Fig. 1a). In the second case (after grain growth) the ODF density decreases around the orientation {111}<112> and increases around {111}<110> (Fig. 1b). It could be simplified using the concept of texture components. A component is defined as an ideal orientation g_i and its associated weight, w_i, calculated as the integral of the ODF around the orientation g_i. In our case the surrounding of an ideal orientation consists of a sphere centered on g_i and with a radius of 15°. With such a definition the components C1 ({111}<110>) and C2 ({111}<112>) have a weight 24.1% and 17.7%, respectively, in the initial state (end of primary recrystallization) and a weight 26.3% and 14.3% after grain growth.

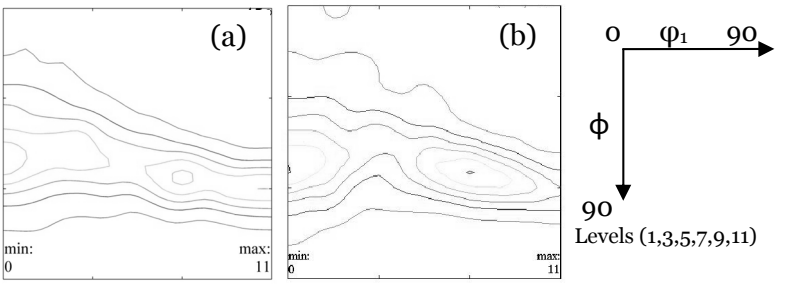

Fig. 1. φ_2 = 45° sections of the ODF for: (a) experimental initial state (630°C, 3 h); (b) experimental finale state (800°C, 5 h).

4.2. Simulated grain growth texture

To study the effect of GB mobility on grain growth, many types of mobility were proposed. Table 1 summarizes some key parameters for the different simulation cases, such as the ODF maximum, the intensities of {111}<110> and {111}<112> components and their weights.

Table 1: Texture features of the cases studied_(the maximum of ODF, ODF densities and weights of the two components {111}<110> and {111}<112>)

	Exp. states		**Simulation : 1st case**				**Simulation : 2nd case**			
			M=1		**M=R-S**		**M=0**		**M=0.5**	
	Ini.	**Fin.**	**p=0**	**p=0 .5**	**p=0**	**p=0 .5**	**CSL**	**Σ3**	**CSL**	**Σ3**
Fmax	10.4	11.2	12.5	13.4	12.1	13.1	12.0	11.9	12.5	12.5
F-C1	10.4	11.2	12.5	13.4	12.1	13.1	12.0	11.9	12.5	12.5
F-C2	9.0	6.0	9.9	11.1	9.8	11.0	10.1	9.4	9.2	9.8
w(%)C1	24.1	26.3	26.6	28.0	25.9	27.4	26.1	25.9	26.4	25.8
w(%)C2	17.7	14.3	19	19.7	19.1	19.6	19.0	18.7	18.4	19.6

First case: isotropic GB mobility (M=constant) and a R-S mobility has been introduced in this grain growth simulation through the reorientation probability (Eq. 3). The ODFs have been calculated using the same conditions as previously, where the simulations were stopped when the mean grain size reached twice the initial value. Figure 2 shows the φ_2=45° sections of grain growth simulations, with isotropic and R-S GB mobilities, for p=0 and p=0.5 respectively (p is the grain size factor). All these ODFs are very similar regardless of the value of p used for the simulation. They resemble rather well the experimental ODF section of the

IF steel after grain growth shown in Fig. 1b. Nevertheless the decrease of the ODF density around {111}<112> is less marked than in the experimental case. In these simulations the weight of the component C1 increases slightly and reaches a level which corresponds to the reality (see Tab. 1). The simulation with p = 0 gives the lowest increase, in particular for R-S GBs mobility. The weight of the component C2 also slightly increases which is opposite to the experimental trend (see Tab. 1). Simulation with R-S GB mobilities presents also the lowest increase of the weight of component C2. It seems to be the closest to the experimental evolution. When the grain size factor is activated (p=0.5), The ODFs obtained from the isotropic and R-S mobilities are indistinguishable (Figs. 2b and 2c). Therefore, the mobility type has a very limited effect on the texture evolution when considering the grain size parameter.

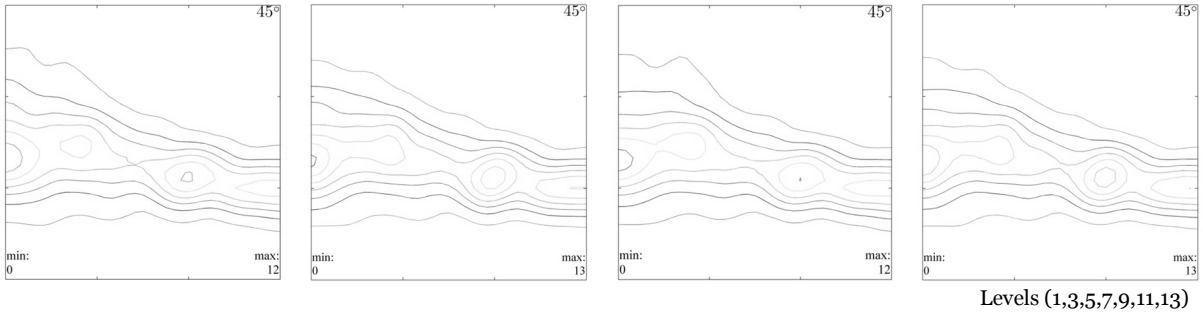

(a) p=0, M=1 (b) p=0.5, M=1 (c) p=0, M(R-S) (d) p=0.5, M(R-S)

Fig. 2: φ_2 = 45° sections of the ODFs obtained from simulations with constant and R-S GB mobility for two values of p (0 and 0.5).

Second case: discrete mobilities for all CSL grains boundaries (all CSL have a unique value of mobility), and separately for only the Σ3 (60°<111>) CSL GB, were incorporated in the R-S function. This calculation assumed that all high angle GBs are equally mobile, except for certain "special" boundaries corresponding to particular misorientation angles (CSL GBs). The mobility values are M=0 and M=0.5. The case M=1 of CSL GB implicitly belongs to the R-S mobility previously studied in the first case. The deviation from the exact CSL misorientation was calculated using Brandon's criterion ($\omega = \pm 15° / \sqrt{\Sigma}$) [24]. The Σ3 CSL GB fraction represents the highest fraction of CSL GBs.
During experimental grain growth, the Σ3 CSL GB frequency increases from 4.30 to 6.32 % while the global CSL GB fraction increases, from 12.88 to 14.71 %. Figure 3 shows the ODF sections of the resulting texture.
These ODFs are quite similar and give the same previous trend (increase of both components in the γ fiber), which may be linked to the weak fraction of the CSL GBs. However, the case M=0 slightly enhances the texture evolution compared to M=0.5. When M=0, the maximum ODF values are 12.0 and 11.9 for all CSL GB and Σ3 GB simulations, respectively.

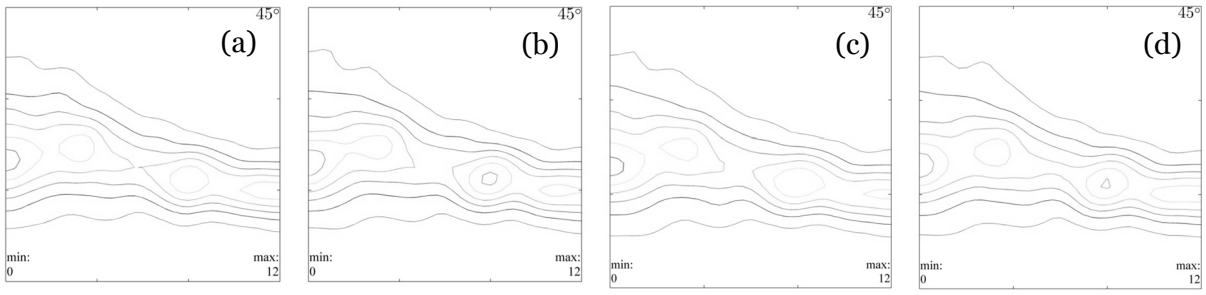

Fig. 3: φ_2 = 45° sections of the ODF's obtained from simulations for: (a) all CSL GBs with M=0; (b) all CSL GBs with M=0.5 ; (c) Σ3 GBs with M=0.5 ; (d) Σ3 GBs with M=0.5.

5. Conclusions

The capability of a modified Potts model to reproduce the experimental grain growth texture of an IF steel has been checked. The following conclusions are obtained from the proposed model which incorporates various GB mobilities:

1) simulations with p=0 for constant and R-S GB mobilities globally give the same features of the experimental texture. Texture obtained with R-S GB mobilities is closest to the experimental evolution. It presents the lowest increase of the weight of the component {111}<112>;
2) the mobility type has a very limited effect on texture evolution when the grain size factor is activated ;
3) texture is slightly enhanced when considering a very low mobility for CSL GBs, in particular for Σ3 GBs.

6. References

[1] Juntunen P, Raabe D, Karjalainen P., Koio T and Bolle G 2001 *Met. Mater. Trans.* A **32** 1989–1995
[2] Magnusson H, Jensen DJ and Hutchinson B 2001 *Scripta Mater.* **44** 435-441
[3] Nakamichi H, Humphreys FJ, Brough I 2008 *J. Microscopy* **230** (3) 464-471
[4] Samet-Meziou A, Etter AL, Baudin T, Penelle R 2008 *Mater. Sci. Eng.* A **473** 342-354
[5] Réglé H, Grandemange D, Miroux A, Bacroix B 2002 *Mater. Sci. Forum* **408-412** 451-456
[6] Samajdar I, Verlinden B, Van Houtte P, Vanderschueren D 1997 *Mater. Sci. Eng.* A **238** 343-350
[7] Miodownik MA 2002 *J. Light Met.* **2** 125-135
[8] Humphreys FJ 2000 *Model. Simul. Mater. Sci. Eng.* **8** 893-910
[9] Ayad A, Rouag N 2012 *Mater. Sci. Forum* **715-716** 872-876
[10] Fjeldberg E, Marthinsen K 2010 *Comp. Mater. Sci.* **48** 267-281
[11] Ivasishin M, Shevchenko V, Vasiliev L, Semiatin L 2006 *Mater. Sci. Eng* .A **433** 216-232
[12] Francis AJ, Roberts G, Cao Y, Rollett AD, Salvador PA 2007 *Acta Mater.* **55** 6159-6169
[13] Ayad A, Wagner F, Rouag N, Rollett AD 2013 *Comp. Mater. Sci.* **68** 189-197
[14] Grest GS, Srlolovitz DJ, Anderson MP 1985 *Acta Metall.* **33** 509
[15] Rollett AD, Srlolovitz DJ, Anderson MP 1989 *Acta Metall.* **37** 1227
[16] Holm EA, Hassold GN, Miodownik MA 2001 *Acta Mater.* **49** 2981
[17] Hayakawa Y, Muraki M, Szpunar JA 1998 *Acta Metall.* **46** 1063
[18]Humphreys FJ, Hatherley M 2002 Recrystallization and Related Annealing Phenomena, Elsevier Publishing Company
[19] Brahme AP 2005 Modelling Microstructure Evolution during Recrystallization *Ph.D. Thesis* Carnegie Mellon University
[20] Brahme A, Fridy J, Weiland H, Rollett AD 2009 *Model. Sim. Mater. Sci. Eng.* **17** 015005
[21] Winning M, Rollett AD, Gottstein G, Srolovitz DJ, Lim A, Shvindlerman LS 2010 *Philos. Mag.* **90** 3107–3128
[22] Ono N, Kimura K, Watanabe T 1999 Acta Mater. **47** 1007–1017
[23] Ayad A, Allain-Bonasso N, Rouag N, Wagner F 2012 *Mater. Sci. Forum* **702-703** 269-272
[24] Brandon DG 1966 *Acta Metall.* **14** 1479-84